ABSTRACT

Title of thesis: Potential Predictability of 500 mb Geopotential Heights on both Monthly and Seasonal Scales over the Northern Hemisphere

Ramdas Ram Singh, Master of Science, 1989

Thesis directed by: Dr. Jagadish Shukla,
Director,
Center for Ocean-Land-Atmosphere Interactions,
Department of Meteorology.

We have used the technique of analysis of variance to assess the potential predictability of interannual fluctuations of seasonal and monthly mean circulations over the Northern Hemisphere. Observed twice daily 500 mb geopotential heights over the Northern Hemisphere were used for this study. The seasons chosen were summer(JJA) and winter(DJF), and the chosen months were June, July, and August, and December, January, and February. The important points noted are: the interannual variance of winter seasonal means is higher than the interannual variance due to climatic noise by a factor of more than two over low latitudes , Japan, a part of the Asian continent, a part of North America , and almost the

whole Pacific. In summer, this ratio becomes more zonally symmetric than in winter and is noteably higher in summer than in winter in low latitudes. This indicates that the low latitude mean winter flows are potentially less predictable than the low latitude mean summer flows.

The most important point to be noted from this study is that the above ratio is higher by a factor of two in the seasonal mean case than in the monthly mean case. The seasonal means of 500 mb geopotential height field are therefore potentially more predictable than the monthly means. This indicates that the boundary forcings have more control over the circulation on the seasonal time scale than on the monthly time scale.

POTENTIAL PREDICTABILITY OF 500 MB GEOPOTENTIAL HEIGHTS ON BOTH MONTHLY AND SEASONAL SCALES OVER THE NORTHERN HEMISPHERE

By

Ramdas Ram Singh
III

Thesis submitted to the Faculty of the Graduate School
of the University of Maryland in partial fulfillment
of the requirements for the degree of
Master of Science
1989

Advisory Committee:

Professor Jagadish Shukla, Advisor
Professor Anandu Vernekar
Dr. Huug van den Dool

To my Mother, my Brothers, my Wife

and the memory of my Father

ACKNOWLEDGEMENTS

Foremost, I would like to express deep gratitude to my Father, Mother, and Brothers, without whose moral and financial support this thesis would never have been come out. Secondly, I wish to graciously acknowledge and personally thank my advisor Prof. Jagadish Shukla, whose great guidance and real help from the beginning I joined this campus has made graduate school a truly learning experience. I would also like to thank the members of the committee, Prof. Anandu Vernekar and Dr. Huug van den Dool.

Special thanks go to Dr. Suranjana Saha, all the members of COLA, my wife, Sunita, and my other friends who gave me moral supports to survive at the time of crisis. Many-many thanks go to both Dr. David Straus who made the very critical review to improve the thesis and to Mr. Daniel Paolino who supplied the data for this study.

TABLE OF CONTENTS

SECTION 1 : INTRODUCTION

There is a growing belief among the community of atmospheric scientists that although it is difficult to make useful instantaneous prediction beyond few weeks (Lorenz, 1965) (because of the inevitable growth of small errors in the initial state of the atmosphere and the use of imperfect models), it is possible to make useful predictions of the overall character of the circulation over some finite interval of time, such as a month or a season. Here interest lies in exploring such a possibility on both monthly and seasonal time scales. This is examined for the winter months of December, January, and February, and the summer months of June, July, and August. The seasonal means chosen are winter(DJF) and summer(JJA).

The difficult task is to distinguish between the low frequency signal generated due to year-to-year variability in seasonal means and the high frequency climate noise produced by day-to-day weather. Such low frequency signals may in part be due to variations in sea surface temperature, changes in snow cover, sea ice extent, and soil moisture (Shukla,1981). We would like to clarify that the objective of this article is not to find out the specific source which causes such a signal but rather to find out if such a signal is statistically significant from the climate noise.

The literature now contains several studies on the potential predictability of the atmosphere, including Madden(1976), Shukla and Gutzler(1983), Nicholls(1981,1983), Trenberth(1984a, 1984b, 1985a, 1985b), Chervin(1986), and Zwiers(1987). The basic approach is an analysis of

variance suggested by Jones(1975). Madden used sea level pressure over the Northern Hemisphere and concluded that the smallest ratio of the interannual variability of climate noise to the actual signal occurred in middle latitudes, between 40^0 N to 60^0 N. The interannual variability of the signal exceeded the climate noise variability north of 60^0 N and south of 40^0 N. Finally, he made the statement that these additional variances may be unpredictable. From 1976 to 1982 Madden was either thought to be correct or little attention was paid to his bold conclusion. In 1983 Shukla pointed out that the method used by Madden(1976) tends to overestimate the natural variability and therefore underestimates the potential predictability. In particular Shukla(1983) criticized Madden's assumption that the potentially predictable climatic signal resides only in frequencies lower than $(96 \text{ days})^{-1}$ and above white noise. Shukla argued that predictable changes due to boundary forcing could occur over periods shorter than a season (such as a month).

Shukla and Gutzler(1983) considered the Northern Hemisphere 500 mb geopotential heights and found that the monthly mean signal stands out significantly from the climate noise over a substantial fraction of the hemisphere during the winter. Nicholls(1981) estimated the potential predictability of surface pressure and temperatures at two Australian stations, Darvin and Adelaide. Nicholls(1983) further considered the surface temperatures at 19 Australian stations and found that the potential predictability was significant mainly over the northern fringes of Australia, in the tropics. Trenberth(1985a, 1985b) assesed the potential predictability on seasonal time scales by considering the 1000 and 500 mb geopotential height fields

over the Southern Hemisphere for both summer and winter, and concluded that the interannual variability clearly exceeds the noise levels at both levels and in both seasons over Antartica and in the tropics. He also found that the methodology fails over the Australia-New Zealand region where clear interannual signals associated with the Southern Oscillation and Quasi Biennial Oscillation have been detected.

Chervin(1986) was the first investigator to examin the potential predictability of simulated data. He examined a twenty-year integration of the NCAR GCM, which was run with identical annual cycles and no interannual variability in ocean surface temperature, snow cover, soil moisture or sea ice. In such data any interannual variability can be attributed solely to internal dynamics. This complete isolation of internal dynamics variability permitted him to make a quantitative comparision of "unpredictable" variance (from the model) and total variance produced by any and all sources (from observational data). The main assumption in such a comparison was that the internal dynamics works in the real atmosphere as it does in the NCAR GCM . This, of course, may or may not be the case. He concluded that no potential predictability was found over the continental United states for mean sea level pressure for any season. In the case of 700-mb geopotential height, a few limited sections of potential predictability were revealed within the primary search area over the Pacific Northwest and the north central states (Minnesota, Wisconsin and Michigan) in summer, and over the southeastern part of the United States in winter.

A similar study was performed using the General Circulation Model of

the Canadian Climate Centre(CCC GCM) as reported by Zwiers(1987). In this integration, the sea surface temperature field was prescribed to follow a climatological seasonal cycle, as was the sea ice and the amount and location of clouds. Zwiers concluded that in the June, July, August(JJA) and September, October, November(SON) seasons there is no evidence of potential predictability, either in the model's surface pressure field or its 500 mb height field. However, there is strong evidence for potential predictability of 500 mb height and surface pressure in the December, January, February(DJF) season and weaker evidence in the March, April, May(MAM) season. This predictability was linked to the occurrence of one single large anomaly extending over a period of about a season.

To best of our knowledge no one has carried out the investigation of potential predictability of seasonal averages using observations over the Northern Hemisphere. Therefore, this article addresses this question. Since we are also interested in comparing the predictability of seasonal means with that of monthly means , the computations for monthly means are also performed.

SECTION 2 : DATA

The data considered for this study are twice-daily (0000 GMT, 1200 GMT) 500 mb geopotential height fields for 20 years, from 1 January 1963 through 31 December 1982, over the Northern Hemisphere between 20° and 90° N. The data are the National Meteorological Center(NMC) archived analyses.

Geopotential height ϕ at any grid point, is expressed as

$$\phi(t) = \overline{\phi} + \sum_{n=1}^{n=N} A_n \cos (\omega_n t) + B_n \sin (\omega_n t),$$

where $\overline{\phi}$ is the 20 year mean, A_n , B_n are Fourier coefficients for frequencies ω_n , $n = 1$ corresponds to a period of 20 years, and $n = N = 7300$ (= 365 x 20) corresponds to a period of one day. The seasonal cycle ϕ_s is defined as the sum of annual (ω_{20}) and semiannual (ω_{40}) components and the 20 year mean, i.e.

$$\begin{aligned} \phi_s(t) = \overline{\phi} &+ A_{20} \cos (\omega_{20} t) + B_{20} \sin (\omega_{20} t) \\ &+ A_{40} \cos (\omega_{40} t) + B_{40} \sin (\omega_{40} t) \end{aligned}$$

where

$$A_{20} = \frac{2}{365 \times 20 \times 2} \sum_{t=1}^{t=365 \times 20 \times 2} \phi(t) \cos (\frac{2 \times \pi \times 20}{365 \times 20 \times 2} t)$$

$$B_{20} = \frac{2}{365\times20\times2} \sum_{t=1}^{t=365\times20\times2} \phi(t) \sin\left(\frac{2\times\pi\times20}{365\times20\times2}t\right)$$

$$A_{40} = \frac{2}{365\times20\times2} \sum_{t=1}^{t=365\times20\times2} \phi(t) \cos\left(\frac{2\times\pi\times40}{365\times20\times2}t\right)$$

$$B_{40} = \frac{2}{365\times20\times2} \sum_{t=1}^{t=365\times20\times2} \phi(t) \sin\left(\frac{2\times\pi\times40}{365\times20\times2}t\right)$$

$$\omega_{20} = \frac{2\times\pi\times20}{365\times20\times2}$$

$$\omega_{40} = \frac{2\times\pi\times40}{365\times20\times2}$$

The anomaly ϕ' at a grid point is defined as

$$\phi'(t) = \phi(t) - \phi_s(t)$$

We have computed the twice daily values of ϕ' at each grid point (4° latitude x 5° longitude) between 20° N and 90° N for 20 years but only 0000 GMT values are used for computations.

SECTION 3 : METHODS

The methodology is very similar to that of Trenberth(1985a,1985b), with the differences to be discussed below. It is supposed that the data base consists of the K daily values that make up the same season for J years in which the mean and annual cycles have been removed. The problem is to assess whether there is any significant climatic variability beyond that due to climatic noise.

For each year, seasonal mean is computed as

$$\bar{x}_j = \frac{1}{K} \sum_{i=1}^{i=K} x_{ij} \tag{1}$$

where x_{ij} is the i^{th} value of the j^{th} sample.

The sample interannual variance ${S_m}^2$ is computed from the data as follows:

$${S_m}^2 = \frac{1}{J} \sum_{j=1}^{j=J} {\bar{x}_j}^2 \tag{2}$$

and an unbiased estimate of the population interannual variance ${\sigma_m}^2$ is

$${\sigma_m}^2 = \frac{J}{J-1} \; {S_m}^2 = \frac{1}{J-1} \sum_{j=1}^{j=J} {\bar{x}_j}^2 \tag{3}$$

assuming $\bar{x}_j$ (j = 1,... J) are independent.

This is a measure of any climatic signal that might exist, but it is combined with variance due to climatic noise.

The intraseasonal sample variance for the j^{th} year is computed as

$$s_j^2 = \frac{1}{K}\sum_{i=1}^{i=K} (x_{ij} - \bar{x}_j)^2 \qquad (4)$$

Then

$$s^2 = \frac{1}{J}\sum_{j=1}^{j=J} s_j^2 \qquad (5)$$

is the mean intraseasonal variance.

The variance due to climatic noise σ_K^2 ,

$$\sigma_K^2 = \frac{\sigma^2}{K_{eff}} = \frac{\sigma^2 T_0}{K} \qquad (6)$$

where K_{eff} is the effective number of independent observations and T_0 the time between independent samples, and is given by

$$T_0 = 1 + 2 \sum_{L=1}^{L=K} (1 - \frac{L}{K}) r_L$$

Here r_L is the autocorrelation at lag L. If it is assumed that our time series can be characterised by a first order autoregressive (" red noise ") process,

then T_0 is given by

$$T_0 = 1 + 2 \sum_{L=1}^{L=K} (1 - \frac{L}{K}) r_1{}^L \qquad (7)$$

where r_1 is autocorrelation at lag 1. We do not consider higher order autoregressive processes in fitting the data in order to calculate T_0 , as Trenberth(1985a,b) does.

The estimation of autocorrelation is carried out as follows. The sample autocovariences at lag L, C_L, are computed as

$$C_{Lj} = \frac{1}{K} \sum_{i=L+1}^{i=K} (x_{i-Lj} - \bar{x}_j)(x_{ij} - \bar{x}_j)$$

where $\bar{x}_j$ are defined in Eqn. 1. is the mean of the obeservations over a season. Similarly the variances C_{0j} are computed for each season. This corresponds to Trenberth's(1984a) " Method A " and may lead to spuriously negative autocovariance at intermediate lags. Trenberth(1985a,b) employs " Method B ", in which only the overall seasonal mean is used. However, we felt that in order to remove the effects of the signal in the calculation of T_0 , which is supposed to characterize the noise, it was justified to remove each seasonal mean separately.

Then the autocorrelations are computed as

$$r_{Lj} = \frac{C_{Lj}}{C_{0j}}$$

Then the overall autocorrelations are

$$r_L = \frac{1}{J}\sum_{j=1}^{j=J} r_{L,j} \tag{8}$$

In order to be a true measure of the noise , the σ^2 in (6) and the T_0 in (7) must exclude any effect of the signal. An unbiased estimate of σ^2 based solely upon the intraseasonal variance (Trenberth, 1984b, c) is

$$\sigma^2 = \frac{K}{K-T_0}\, s^2 \tag{9}$$

Therefore , from (6) and (9)

$$\sigma_K{}^2 = \frac{T_0}{K-T_0}\, s^2 \tag{10}$$

Now we form the F ratio as

$$F = \frac{\sigma_m{}^2}{\sigma_K{}^2} \tag{11}$$

is the ratio of the two estimated interannual variances and it should follow the F distribution with $J-1$ and $J(K_{eff}-1)$ degrees of freedom.

If this ratio is greater than F_c then the signal is supposed to be potentially predictable. If T_0 is 5.0 then for 99% level of significance, the F_c is 2.0 for both winter and summer seasons where as for winter and summer months the F_c is 2.3.

The main differences between this study and the study by Trenberth(1985) are: a) we assume that the time series is characterised by a first order autoregressive process whereas Trenberth goes for higher order processes. b) in computing autocovariances we remove the seasonal means instead of the mean of all the seasons which was removed by Trenberth.

In the monthly mean predictability cases $\overline{x}_j$ in Equations (3) and (4) become monthly means instead of seasonal means. There is not much difference in computing the characteristic time T_0 from (7) except that K becomes 30. The autocorrelations remain the same as computed for the seasonal mean predictability cases. The final changes are made in (10) where also K becomes 30.

SECTION 4 : RESULTS

The autocorrelations of 500 mb height anomalies at one day lag, calculated from (8), are presented in Figs. 1 and 2 for the winter and summer seasons respectively. The results are in good agreement with those of Gutzler and Mo(1983) for both seasons. From Fig. 1 the important points to be noted are: a) The lowest values of autocorrelation occurs over the mid-latitude east coasts of Asia and North America. This agrees with the facts that these two regions are the "storm track" regions where day-to-day fluctuations are highest. b) The autocorrelations are highest over the polar regions. c) Autocorrelations start increasing in low-latitudes in summer, indicating smaller day-to-day variability than in mid-latitudes. Although the autocorrelation at lags greater than 1 day is not shown here it is noted that in winter the autocorrelation is positive until day 6 and becomes negative at day 7 in mid-latitudes and in the polar regions. This remains true till day 11 and beyond. We found some patches with negative autocorrelations in low latitudes too. The autocorrelations were not computed beyond lag 30. The fact that the autocorrelations become negative may be a result of using separate seasonal means in the calculation of the autocovariances. The autocorrelations over the low latitudes are generally higher than those over midlatitudes for lags greater than one day, indicating a longer memory in the tropics.

In Fig. 2, which depicts the autocorrelations for summer, the general pattern is the same, but the regions of lowest autocorrelation over the east

coasts of Asia and North America have shifted eastward. The autocorrelations start becoming negative at lag 5 near Alaska , the east coast of the United States, over southern Europe, and the northern tip of India. Considering the autocorrelations computed up to lag 30, we can again conclude that the lower latitude atmosphere has a longer memory than the mid- and high latitude atmospheres.

The characteric times T_0 (days) are shown in Figs. 3 and 4 for winter and summer 500 mb height respectively. It is very clear from both figures that the storm track regions (i.e. east coast of Asia and North America) have the lowest values of T_0 . The values are highest in the polar regions and are somewhat higher in low latitudes than in midlatitudes. The characteristic times T_0 (days) for 500 mb. heights for both winter and summer monthly mean cases are presented in Figs. 5 and 6 respectively. It is noted that there is no significant difference between Figs. 3 and 5 and between Figs. 4 and 6.

The winter and summer seasons 500 mb. height daily variances(meters squared) from(5) are shown in Figs. 7 and 8 respectively. (All other variances are also given in meters squared.) The general structure of Fig. 7 agrees well with Fig. 3a of Blackmon(1976). The maxima and minima in Fig. 8 are in phase with the maxima and minima in Fig. 8a of White(1982). The maximum variances occur along 45 °N - 50 °N belt, somewhat downstream of the dominant storm track activity along that latitude belt. The storm track characteristics typical of high frequency baroclinic eddies are mainly found over east coasts of Asia and North America, while the max-

ima in Figs. 7 and 8 over the north-east Pacific and north-mid Atlantic are associated with lower frequency fluctuations such as blocking.

The interannual variances of 500 mb. heights, calculated from (3) for the winter and summer seasons are presented in Figs. 9 and 10 respectively. There is some consistency with the winter results in the positions of the maxima over the Pacific and Atlantic Oceans and over northern Russia. The winter maxima and minima are about five times stronger in magnitude than in summer. This difference in magnitude indicates that the winter circulation is forced differently than the summer circulation. For example, in winter the enhanced land-ocean temperature contrast leads to vigorous stationary waves, which in turn form preferred regions for the development of baroclinic waves. In summer, the weaker land-ocean temperatures contrast is reflected in a less vigorous development of waves.

The intraseasonal noise variance $\sigma_K{}^2$ from (10) is shown in Figs. 11 and 12 for winter and summer respectively. The winter intraseasonal variances are almost double that of the summer intraseasonal variances. The interannual variances for monthly means are presented for winter and summer in Figs. 13 and 14 respectively. The noise variances for these two means are shown in Figs. 15 and 16. It is not surprising that the interannual variance of monthly means is much higher than the interannual variance of seasonal means: the relatively smaller scales represented on maps of monthly means themselves have interannual variability, in addition to the variability of the mean state. The positions of the important features of interannual variance do not change much from the seasonal mean to the

monthly mean time scale .

The F-ratios from(11) for the winter and summer seasons are shown in Figs. 17 and 18 respectively. The tropics has higher F-ratio than the midlatitudes as was revealed in a paper by Shukla and Gutzler(1983). The maxima over the Pacific is in agreement with that of Shukla and Gutzler(1983). From Fig. 17 it can be observed that over almost the whole Pacific, most of the North America, parts of the Asian continent , Japan, and the low latitudes the F values are greater than 2, which corresponds to a significant level at the 99% level of confidence. In summer, regions for which the value of F exceeds 2 extend further into the northern hemisphere and become more zonally oriented. This reflects the fact that the day-to-day fluctuations have less variability along a latitude circle in the summer than the winter. The F values are considerably higher in summer than the winter in low latitudes. This means that on the seasonal scale the low latitude summer is potentially more predictable than the winter. A paradoxical result is that on the seasonal scale the low latitude atmosphere is potentially more predictable than the mid-latitude atmosphere, whereas for day-to-day weather the mid-latitudes are potentially more predictable, as noted by Shukla(1981).

In Figs. 19 and 20 the F-ratios for winter and summer monthly means are presented, respectively. The conclusions drawn from the seasonal mean results remain true, except that the F-ratios have lower values in the monthly mean case. This implies that the seasonal means are potentially more predictable than the monthly means. The reason behind this is con-

jectured as follows. It is believed that the low frequency signals such as the sea surface temperature, changes in snow cover, sea ice extent, and soil moisture are the main sources to give rise the monthly and seasonal means which are considered to be potentially predictable. Since these boundary forcings work on seasonal (and longer) time scales, it is reasonable that the atmospheric response to these forcings is seen more strongly on seasonal than on monthly time scales.

SECTION 5 : SUMMARY AND CONCLUSIONS

The objective of this study is to quantify the interannual and intraseasonal variances of observed 500 mb geopotential heights over the Northern Hemisphere, on both monthly and seasonal scales, and to investigate if the interannual variances significantly exceed the intraseasonal variances. The major conclusions drawn are as follows:

1.) In the seasonal mean case, the winter level of interannual variances is about five times that in summer, although the patterns maintain some consistency. Clearly the winter flows are forced differently than the summer flows.

2.) The winter season F-ratios have values greater than two (indicating statistical significance) over almost the whole Pacific, part of North America, parts of the Asian continent , Japan, and the low latitudes. Over the central Pacific this ratio has the value of four. It is conjectured that this high is related to the warming of central Pacific during El Nino years.

3.) The summer seasonal F-ratios are zonal in structure compared to the winter F-ratios. The maximum of the winter season in the central Pacific disappears in summer, because the anomalous heating of the central Pacific does not occur then.

4.) The summer low latitude F-ratios are much higher than those in winter because of the low day-to-day variability in the low latitude summer. The summer mean low latitude flows are potentially more predictable

than the winter mean flows.

5.) The F-ratios are higher in the low latitudes than in mid-latitudes in both winter and summer seasons, indicating that on seasonal scales the low latitudes are potentially more predictable than the mid-latitudes.

6.) It seems that the high latitudes do not have predictive signals during both winter and summer.

7.) The F-ratios in the seasonal mean cases are in general higher than those in the monthly mean cases. Therefore, seasonal mean atmospheric circulations are potentially more predictable than the monthly mean atmospheric circulations. The reason behind this is that the low frequency signals, which are assumed to be the sources for these two means, can not be captured as much on the monthly mean scale as can be on the seasonal mean scale.

In conclusion, the present work can be expanded in several ways. For example: a) the above computations can be performed for GCMs other than the CCC GCM, such as the Goddard Laboratory for Atmosphere's GCM. This requires a lengthy multi-year simulation. b) one can repeat the present work for the Indian rainfall which extends for almost 100 years. This study can also be performed for ocean fields too.

REFERENCES

Blackmon, M.L., 1976: A climatological spectral study of the 500 mb geopotential height of the Northern Hemisphere. J. Atmos. Sc., 33, 1607-1623

Chervin, R.M., 1986: Interannual variability and seasonal climate predictability. J.Atmos.Sci., 43, 233-251

Jones, R.H., 1975: Estimating the variance of time averages. J. Appl. Meteor., 14, 159-163.

Lorenz, E.N., 1965: A study of the predictability of a 28-variable atmospheric model. Tellus, 17, 321-333

Madden, R.A., 1976: Estimation of the natural variability of time-averaged sea-level-pressure. Mon. wea. rev., 104, 942-952.

Nicholls, N., 1981: Air-sea interaction and the possibility of long-range weather prediction in the Indonesian Archipelago. Mon. Wea. Rev., 100, 2435-2443.

---------, 1983: The potential for longe-range prediction of seasonal mean temperature in Australia. Aust. Meteor. Mag., 31, 203-207.

Shukla, J., 1981: Dynamical predictability of monthly means. J. Atmos. Sci., 38, 2547-2572.

---------, and D. Gutzler, 1983; Interannual variability and predictability of 500 mb geopotential heights over the Northern Hemisphere. Mon. Wea. Rev., 111, 1273-1279.

Trenberth, K.E., 1984a: Interannual variability of the Southern Hemisphere ciculation: Representatives of the year of the Global Weather Experiment. Mon. Wea. Rev., 112, 108-123

---------, 1984b: Some effects of finite sample size and persistence on on meteorological statistics. Part I: Autocorrelations. Mon. Wea. Rev., 112, 2359-2368.

---------, 1984c: Some effects of finite sample size and persistence on meteorological statistics. Part II: Potential predictability. Mon. Wea. Rev., 112, 2369-2379.

---------, 1985a: Persistence of daily geopotential heights over the southern Hemisphere. Mon. Wea. Rev., 113,38-63

---------, 1985b: Potential predictability of geopotential heights over the Southern Hemisphere. Mon. Wea. Rev., 113, 54-64.

White, G.H., 1982: An observational study of the Northern Hemisphere extratropical summertime general circulation. J. Atmos., 39, 24-40.

Zwiers, F. W., 1987: A potential predictability study conducted with an atmospheric General Circulation Model. Mon. Wea. Rev., 115, 2957-2974.

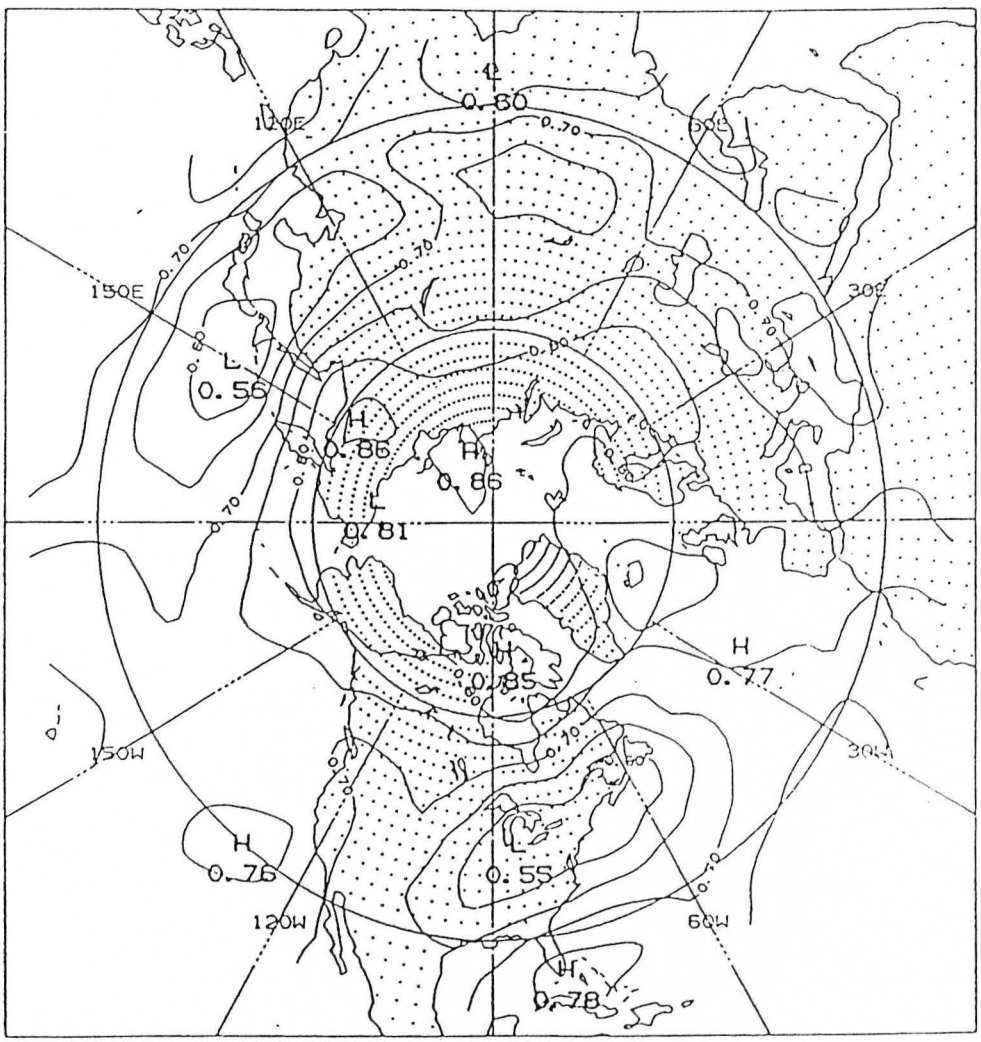

Fig. 1. Autocorrelation of wintertime 500 mb heights lagged by one day, with annual and semiannual cycles removed. Contour interval 0.05.

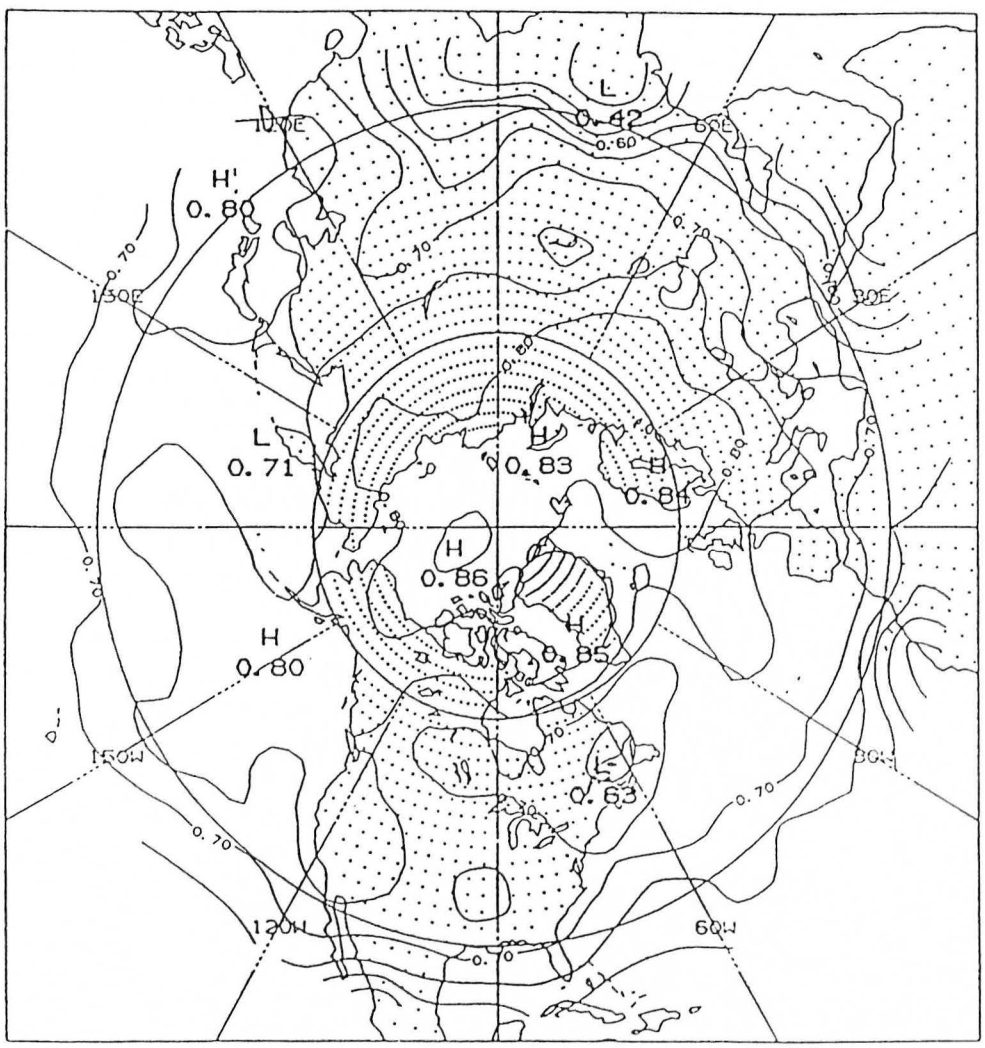

Fig. 2. Autocorrelation of summertime 500 mb heights lagged by one day, with annual and semiannual cycles removed. Contour interval 0.05.

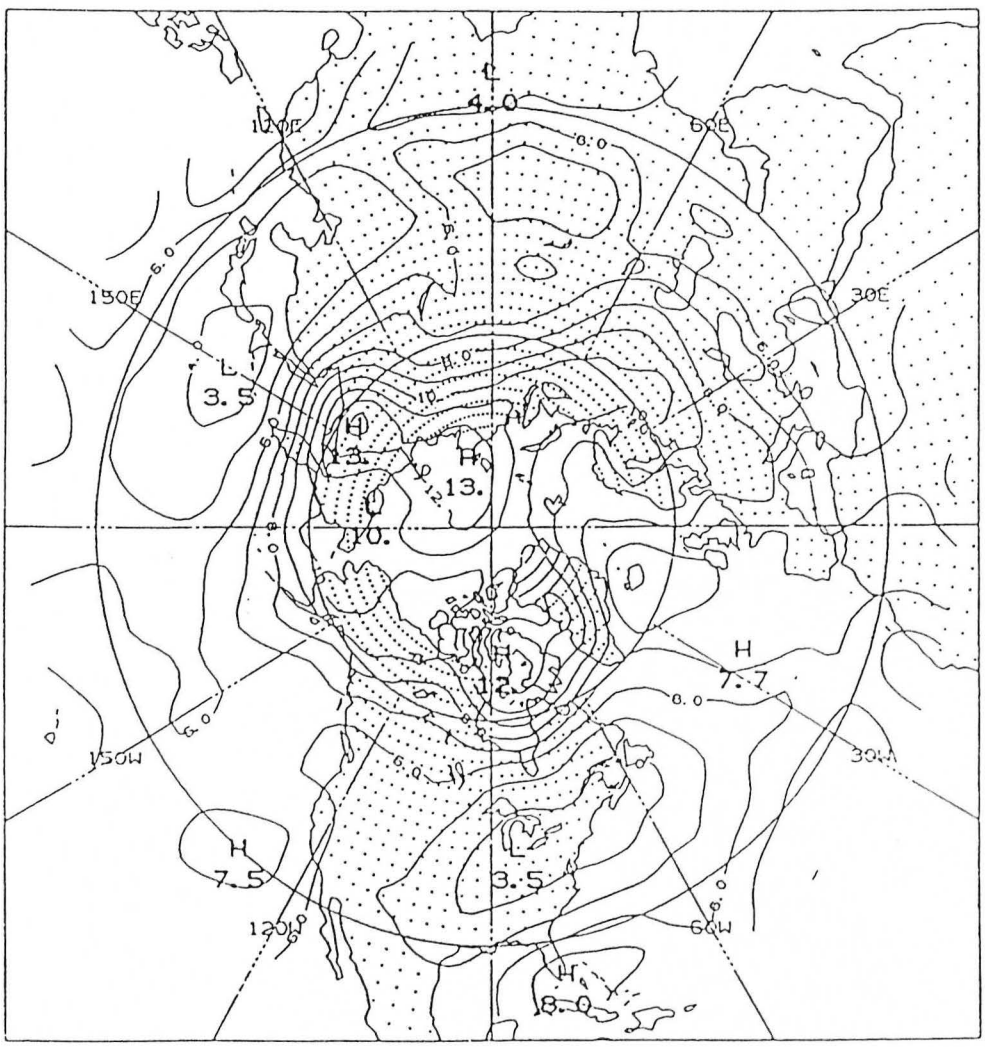

Fig. 3. Estimated time (days) between independent sample of the 500 mb height field for wintertime. Contour interval 1 day.

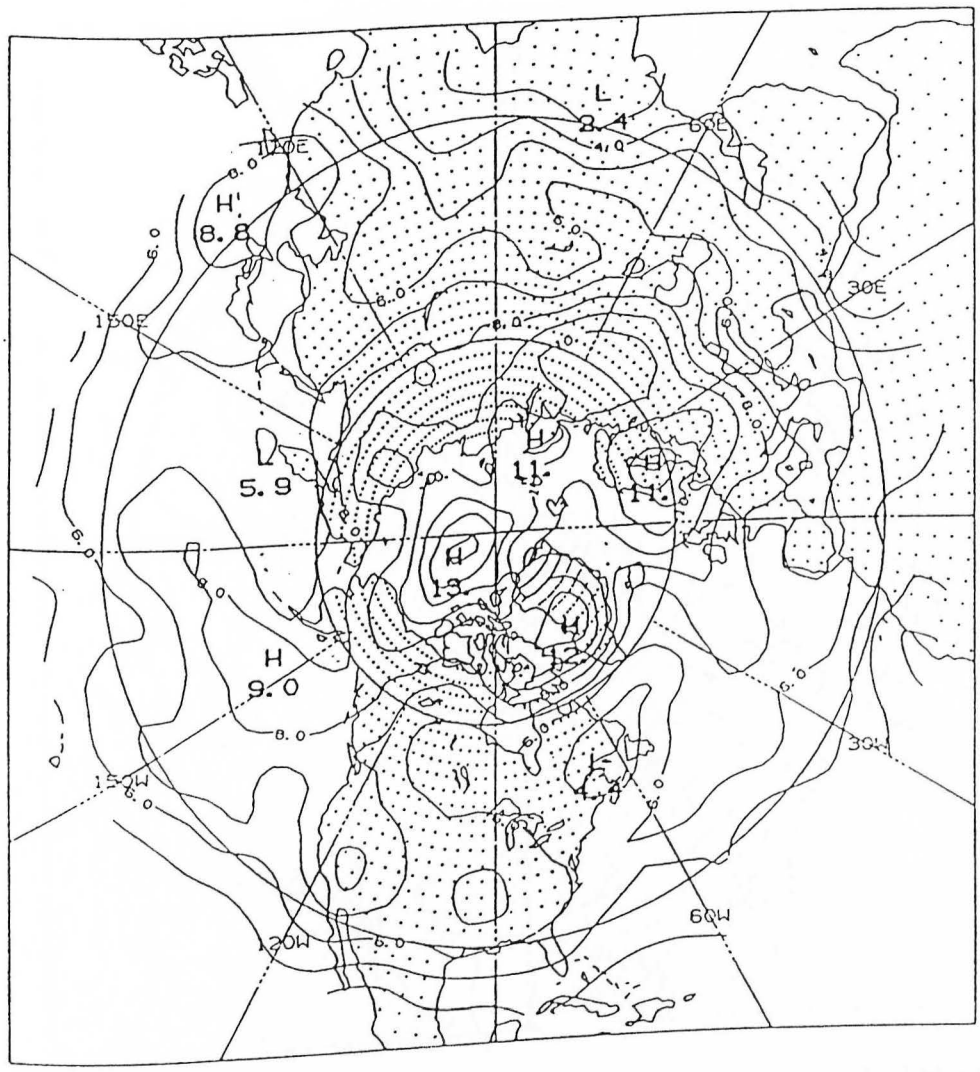

Fig. 4. Estimated time (days) between independent sample of the 500 mb height field for summertime. Contour interval 1 day.

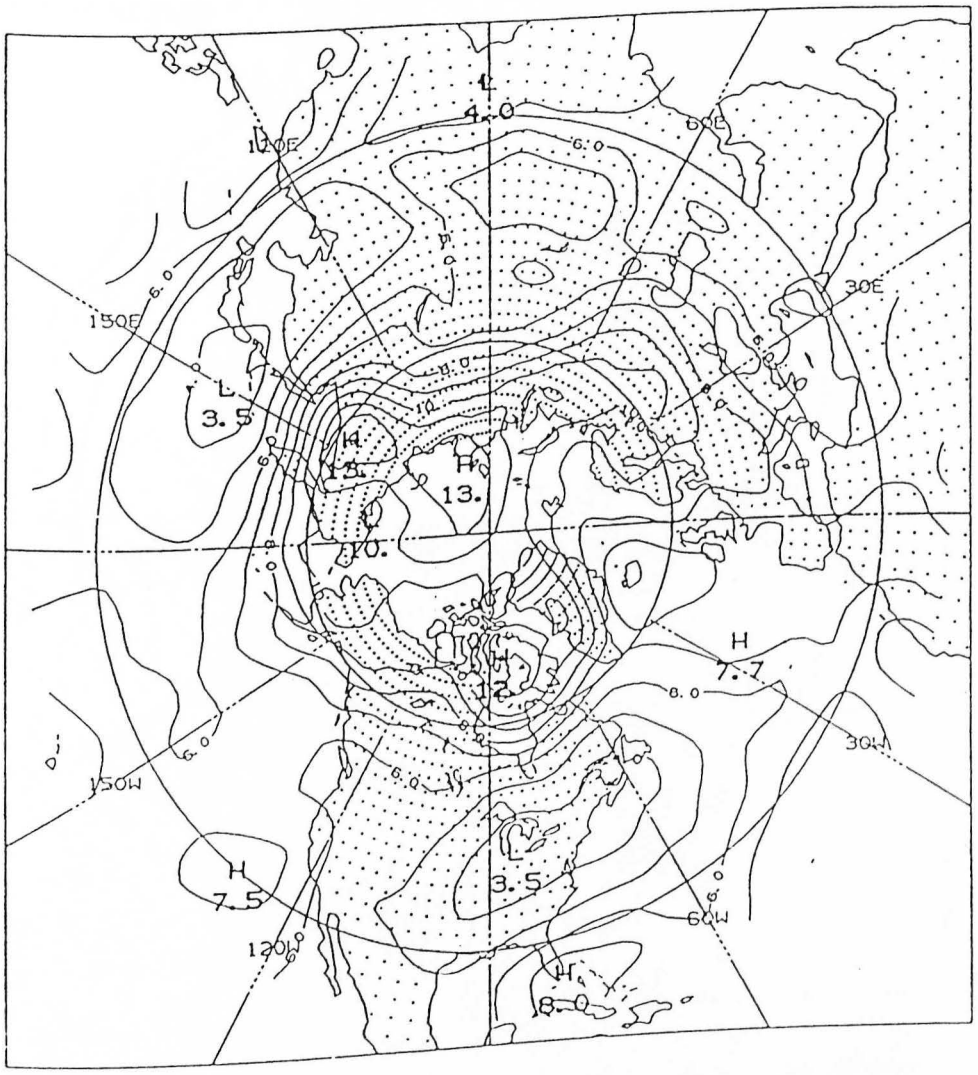

Fig. 5. Estimated time (days) between independent sample of the 500 mb height field for winter months. Contour interval 1 day.

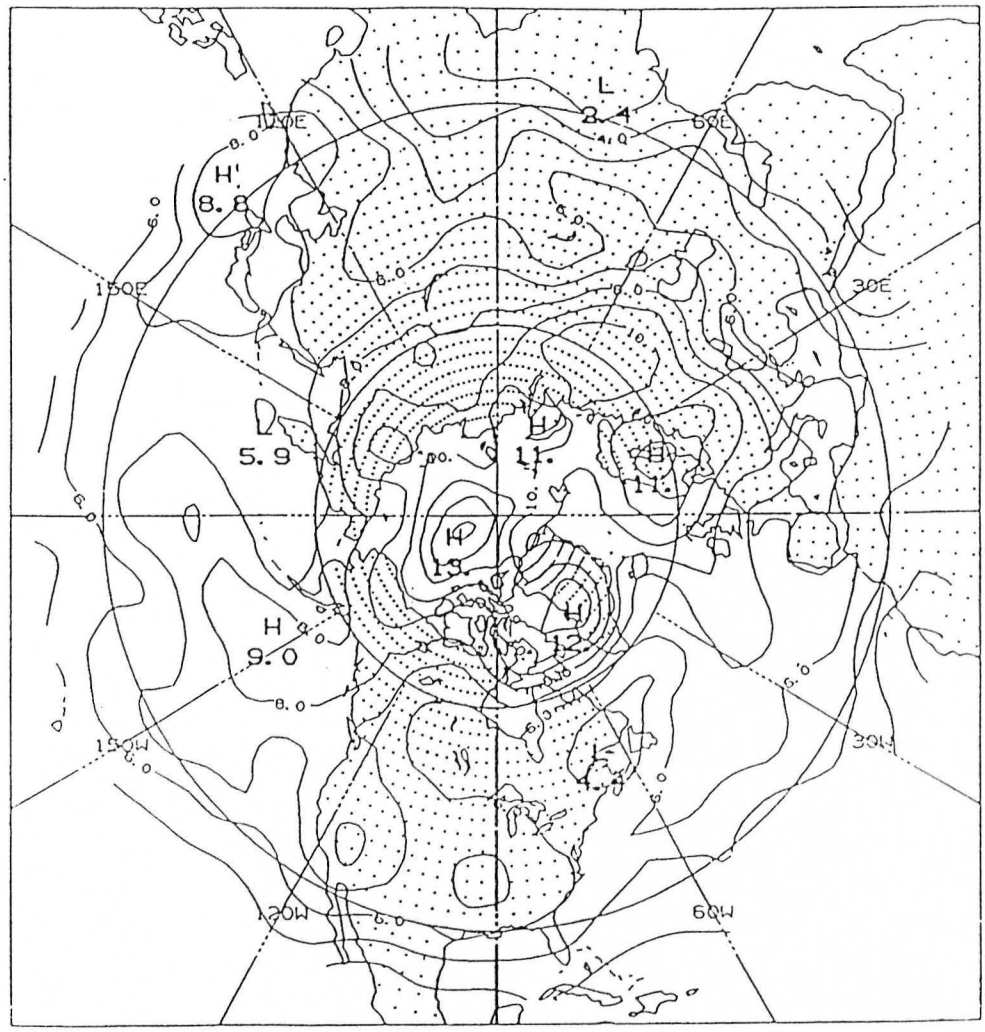

Fig. 6. Estimated time (days) between independent sample of the 500 mb height field for summer months. Contour interval 1 day.

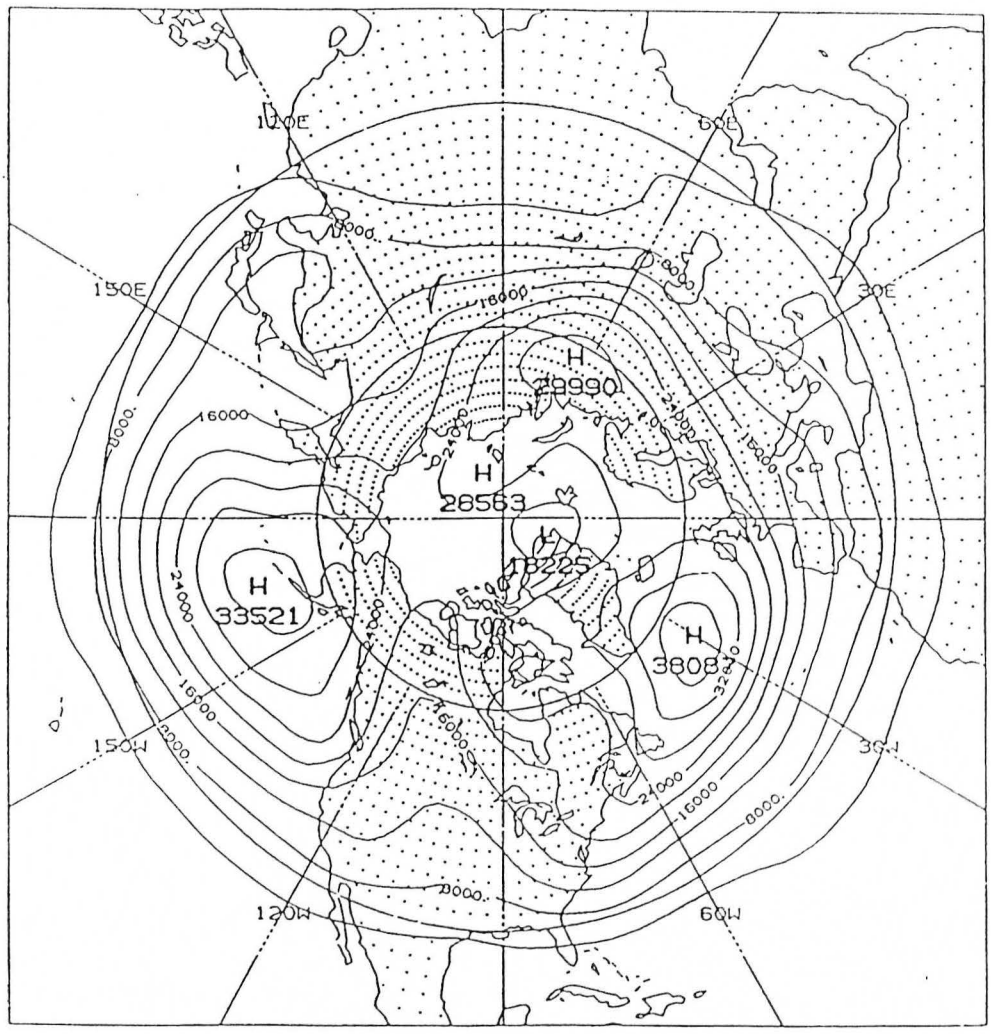

Fig. 7. Sample daily variance of 500 mb heights for winter season. Contour interval 4000.0 meter squared.

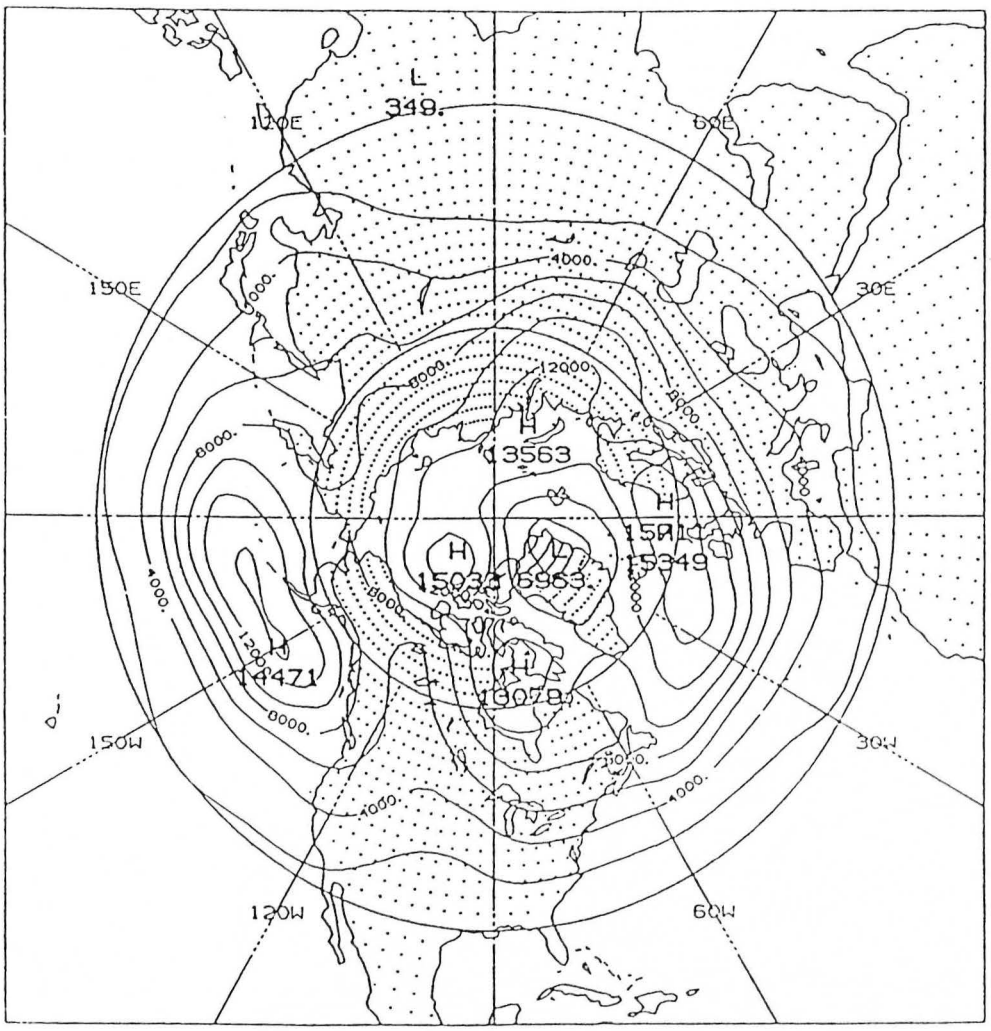

Fig. 8. Sample daily variance of 500 mb heights for summer season. Contour interval 2000.0 meter squared.

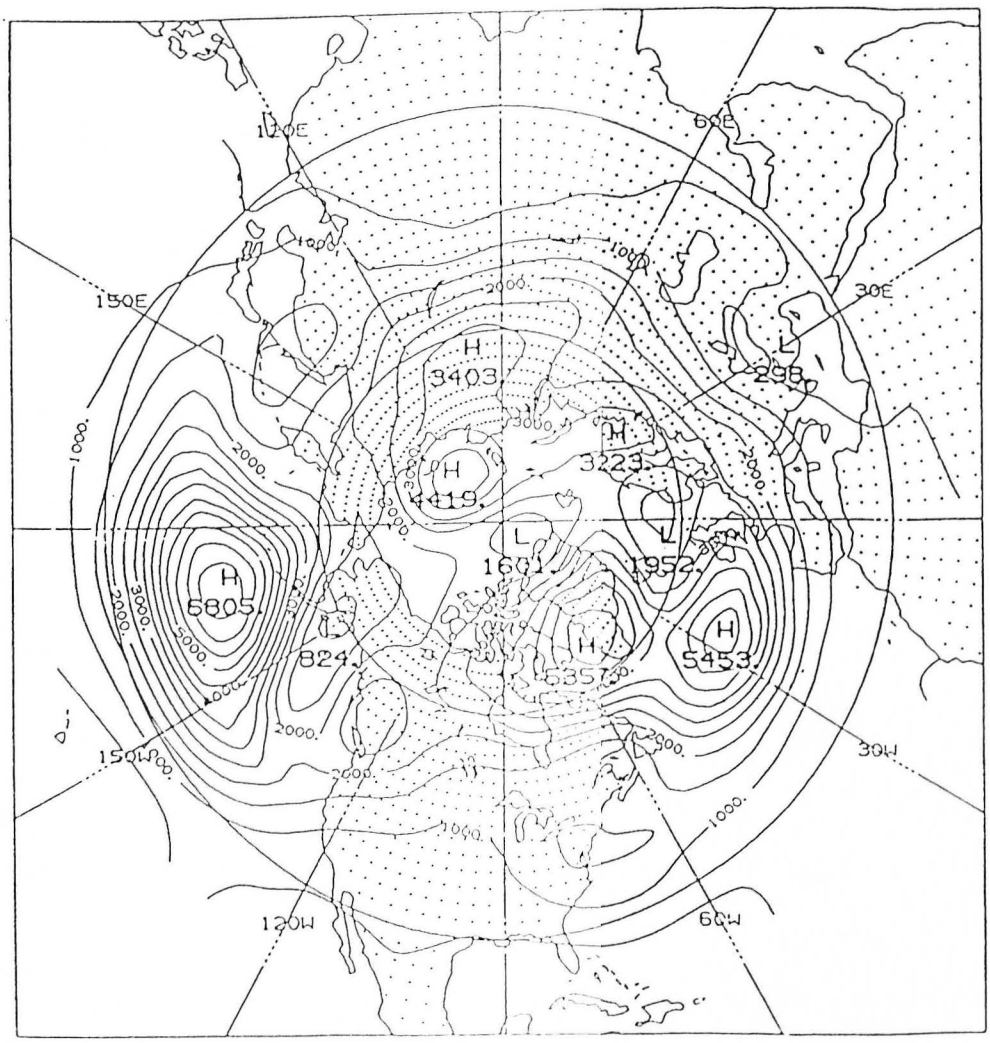

Fig. 9. Interannual variance of winter seasonal means of 500 mb heights.

Contour interval 500.0 meter squared.

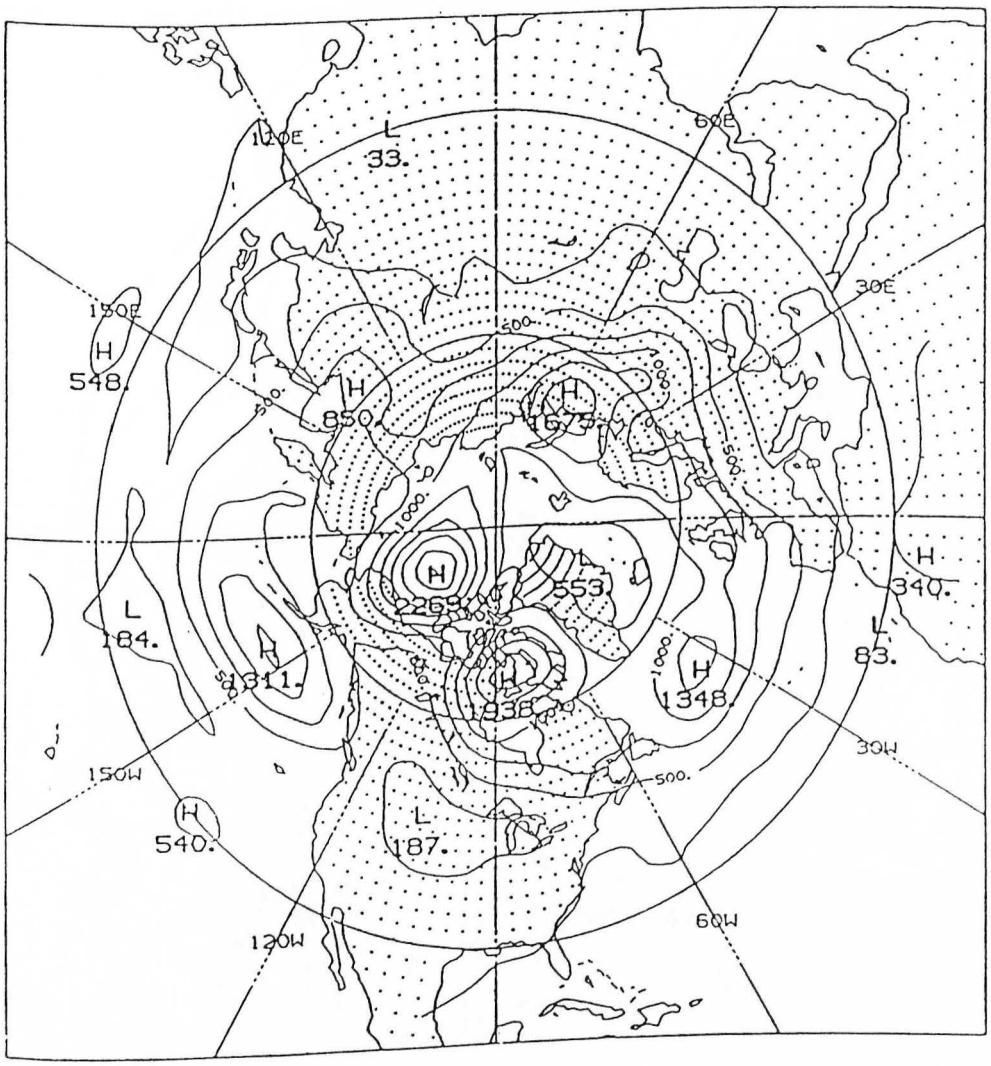

Fig. 10. Interannual variance of summer seasonal means of 500 mb heights. Contour interval 250.0 meter squared.

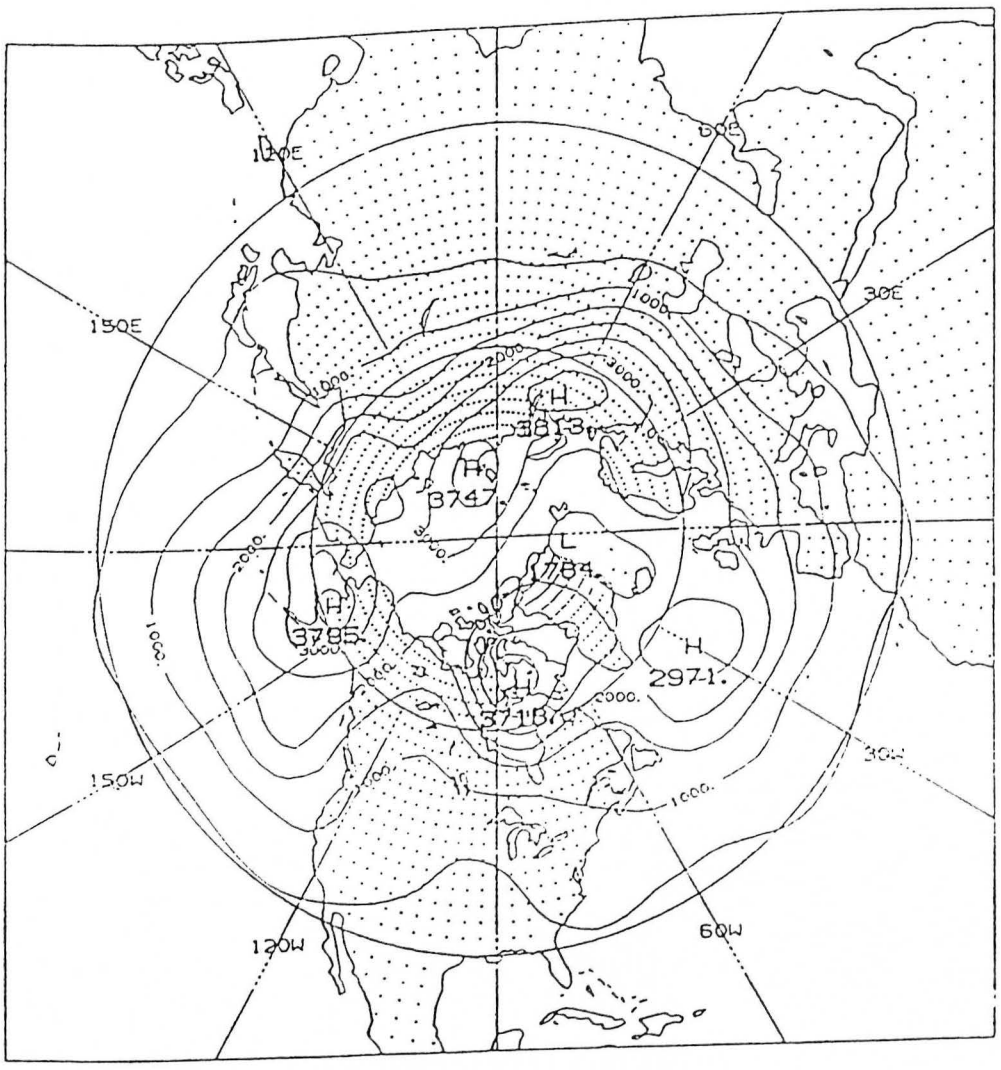

Figure 11: Interannual variance due to climatic noise of winter season 500 mb heights. Contour interval 500.0 meters squared.

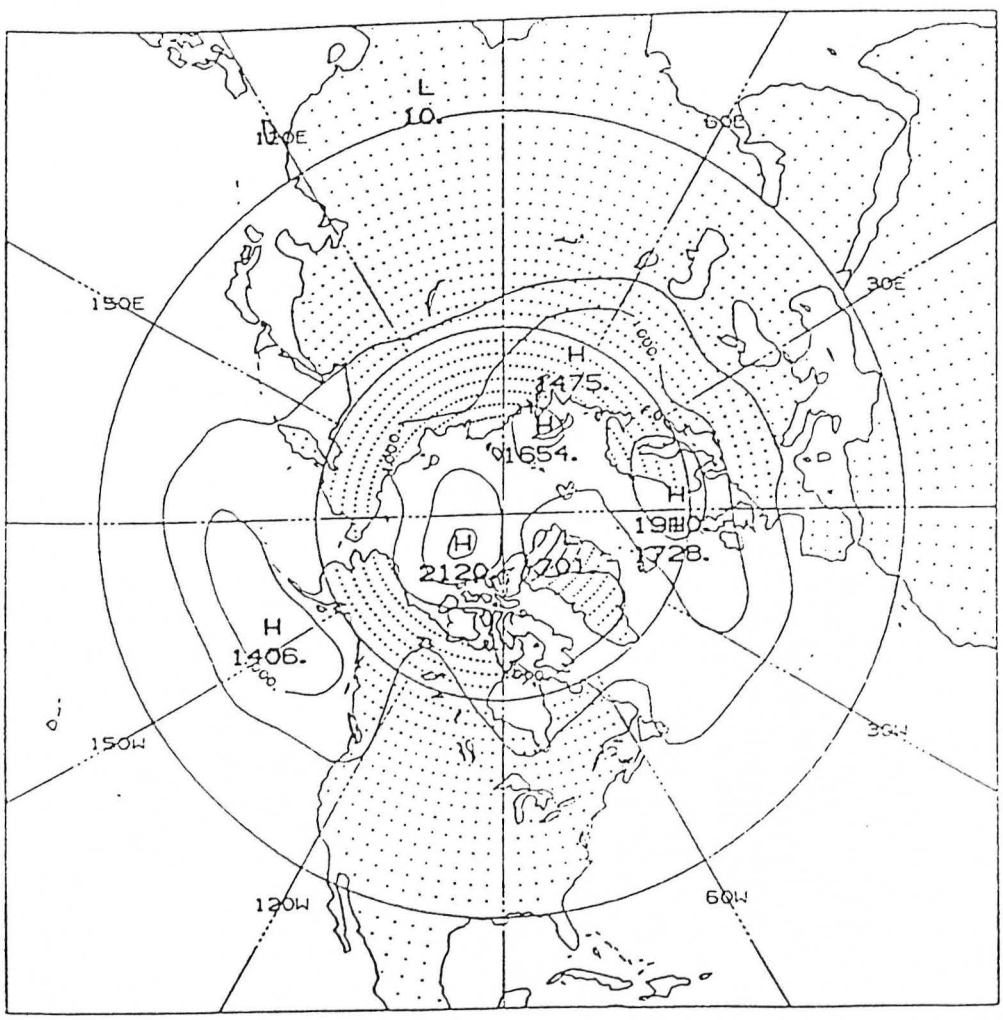

Figure 12: Interannual variance due to climatic noise of summer season 500 mb heights. Contour interval 500.0 meters squared.

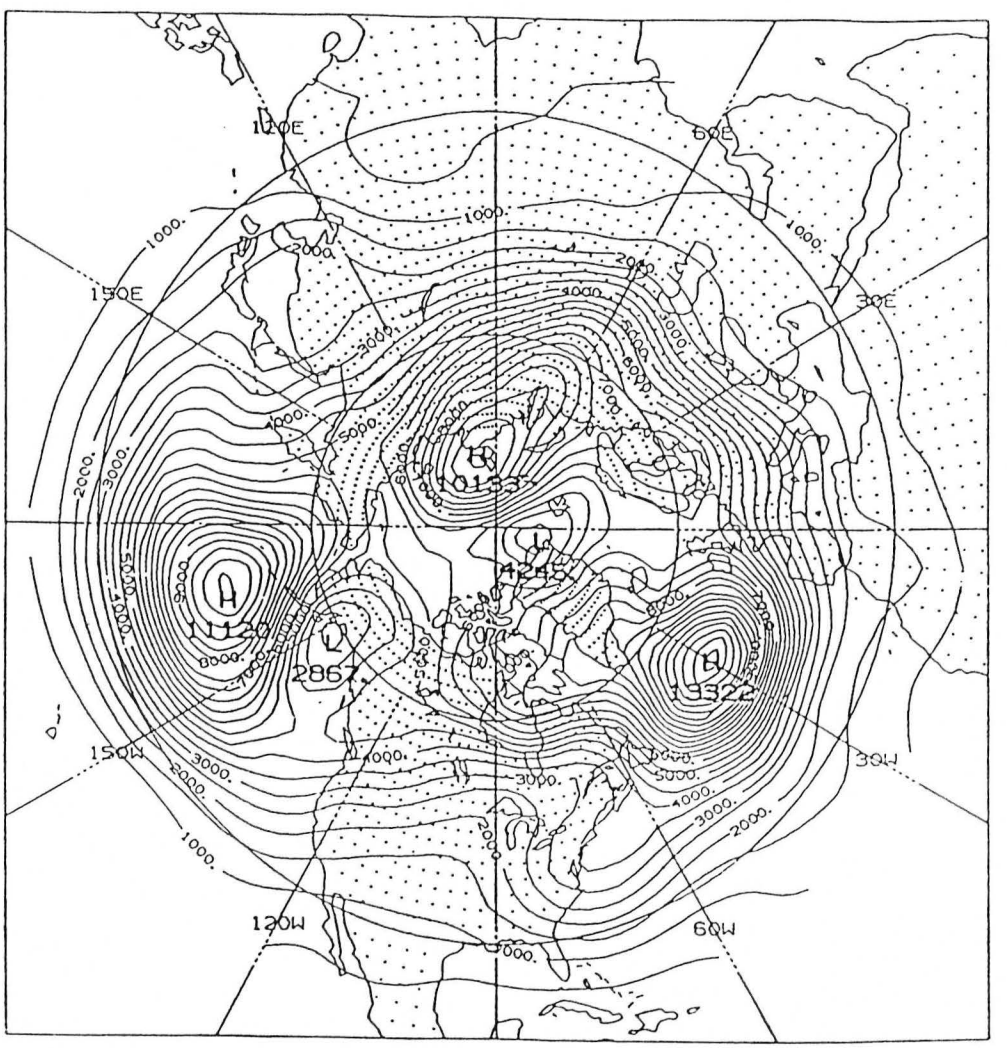

Fig. 13. Interannual variance of winter monthly means of 500 mb heights. Contour interval 500.0 meter squared.

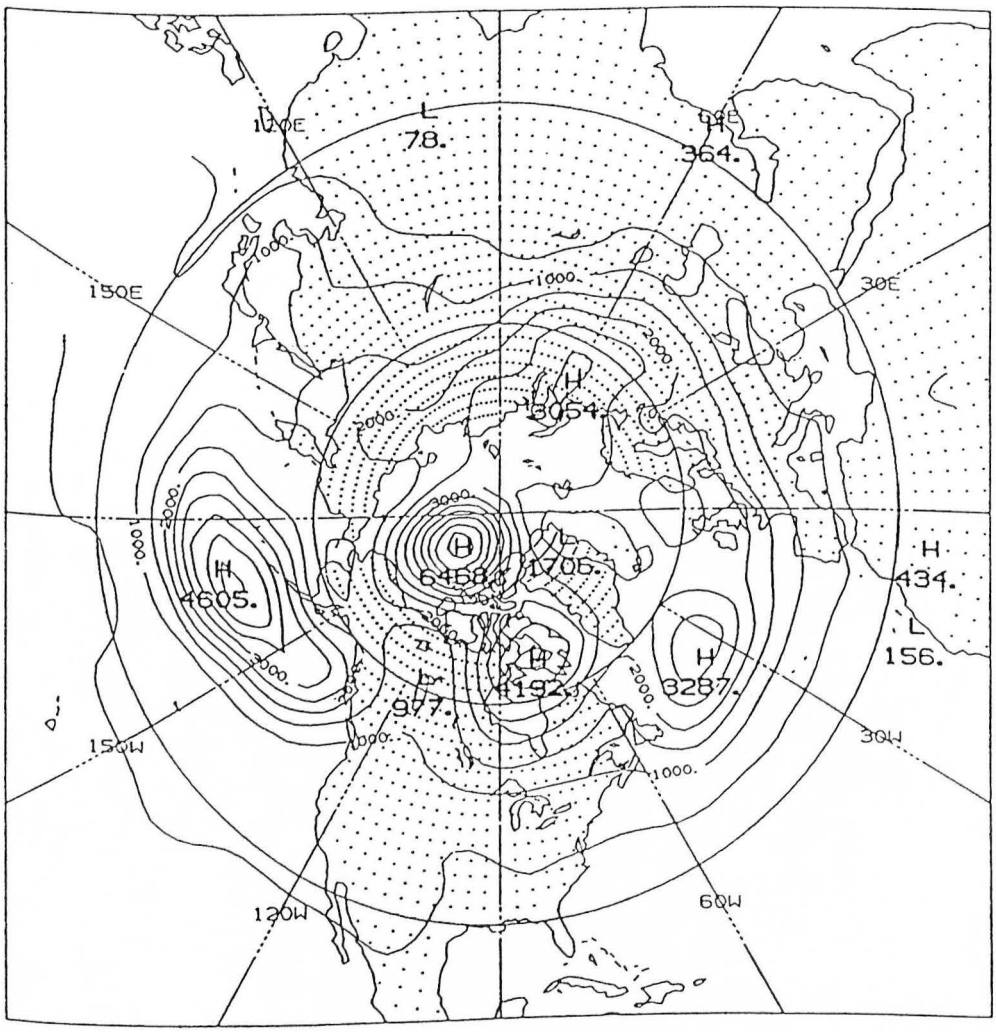

Fig. 14. Interannual variance of summer monthly means of 500 mb heights. Contour interval 500.0 meter squared.

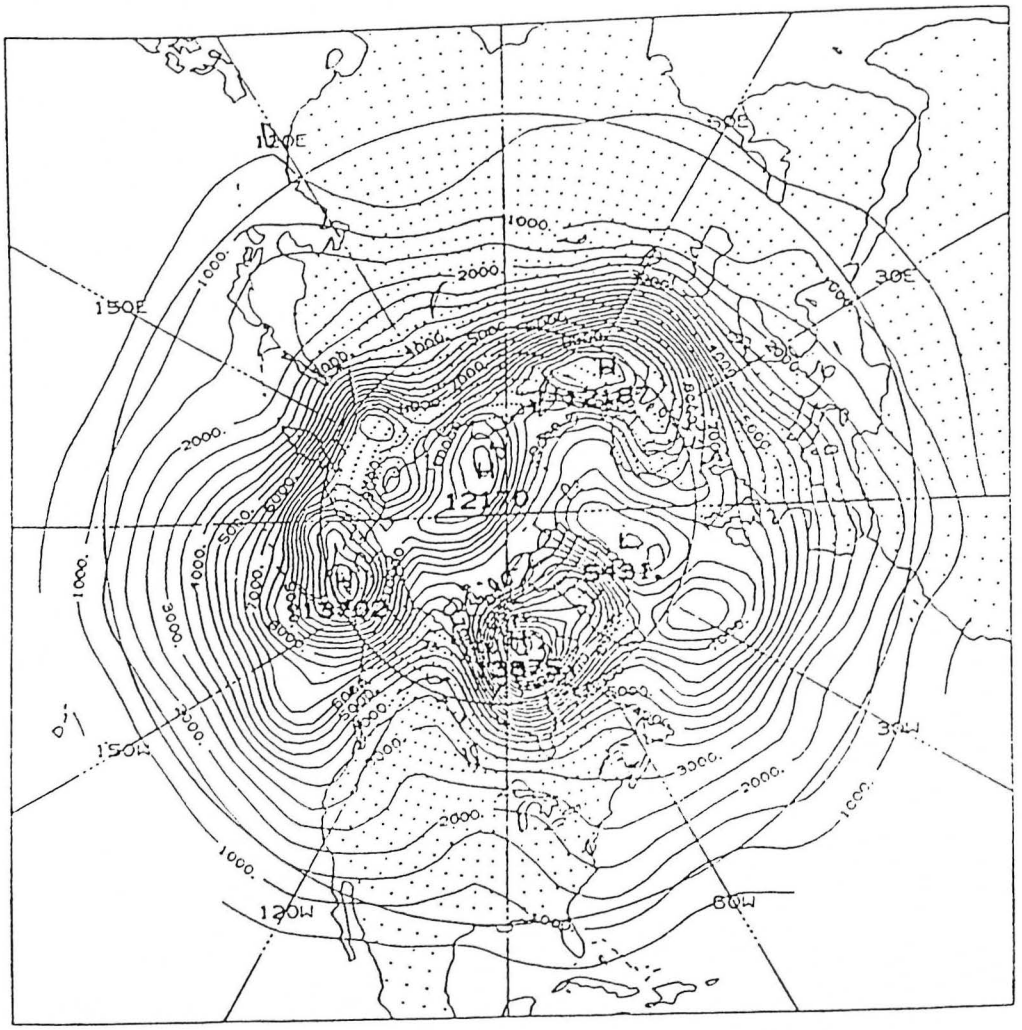

Figure 15: Interannual variance due to climatic noise of winter months 500 mb heights. Contour interval 500.0 meters squared.

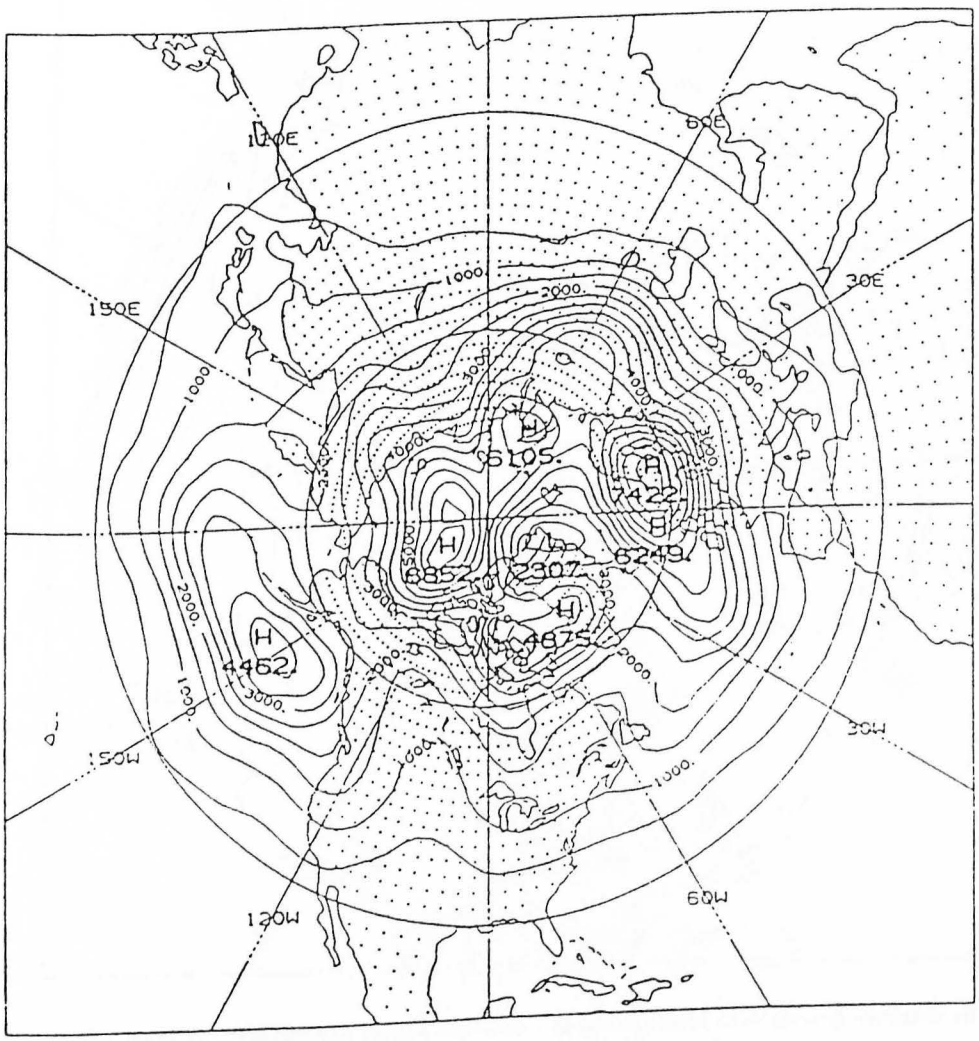

Figure 16: Interannual variance due to climatic noise of summer months 500 mb heights. Contour interval 500.0 meters squared.

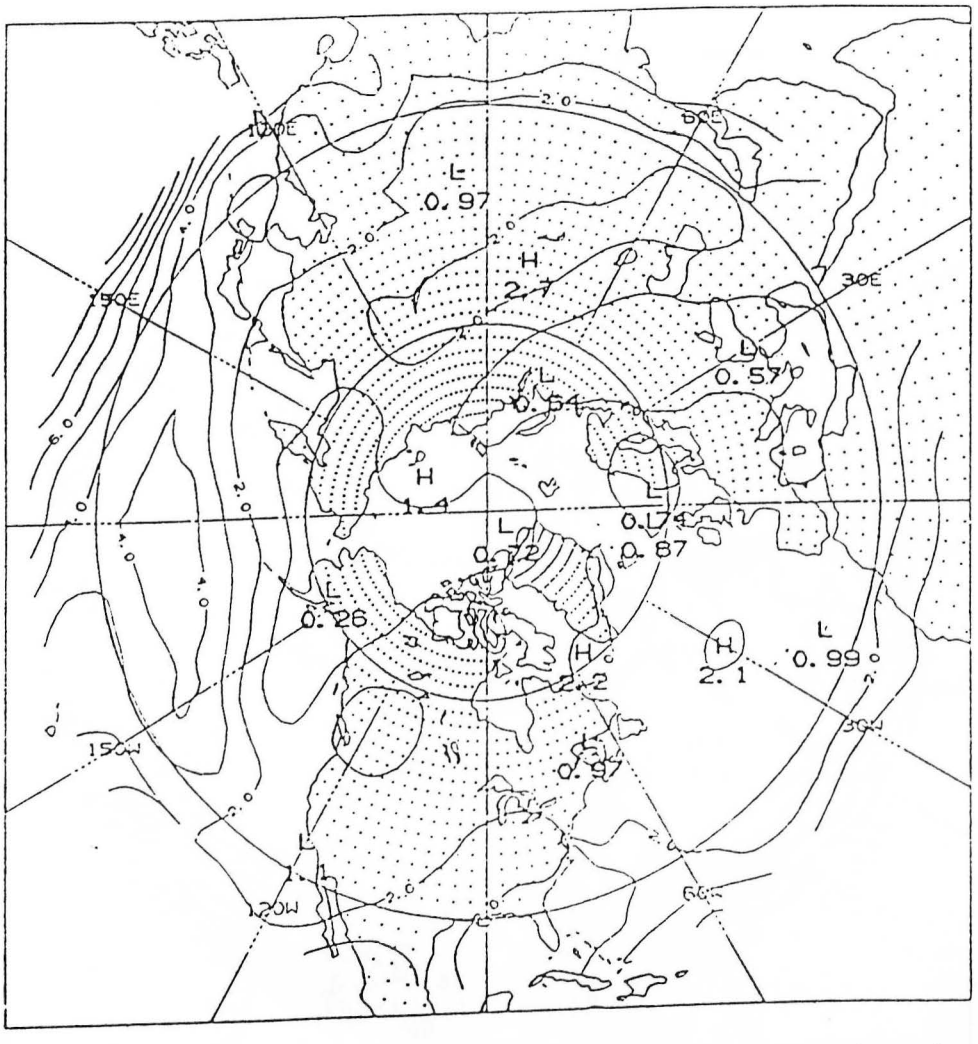

Figure 17: F-statistic values representing the ratio of interannual variance of winter seasonal mean to interannual variance due to climatic noise of winter season. Contour interval 1.0.

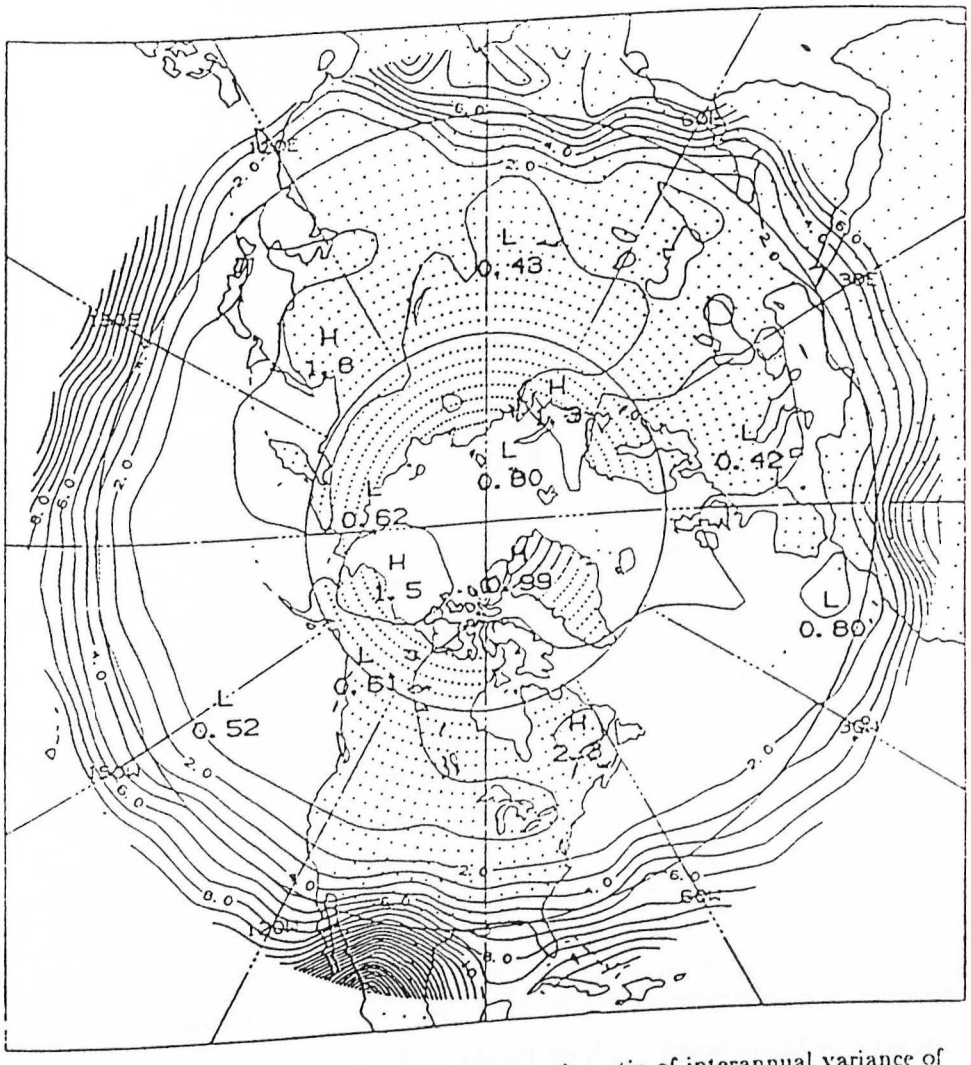

Figure 18: F-statistic values representing the ratio of interannual variance of summer seasonal mean to interannual variance due to climatic noise of summer season. Contour interval 1.0.

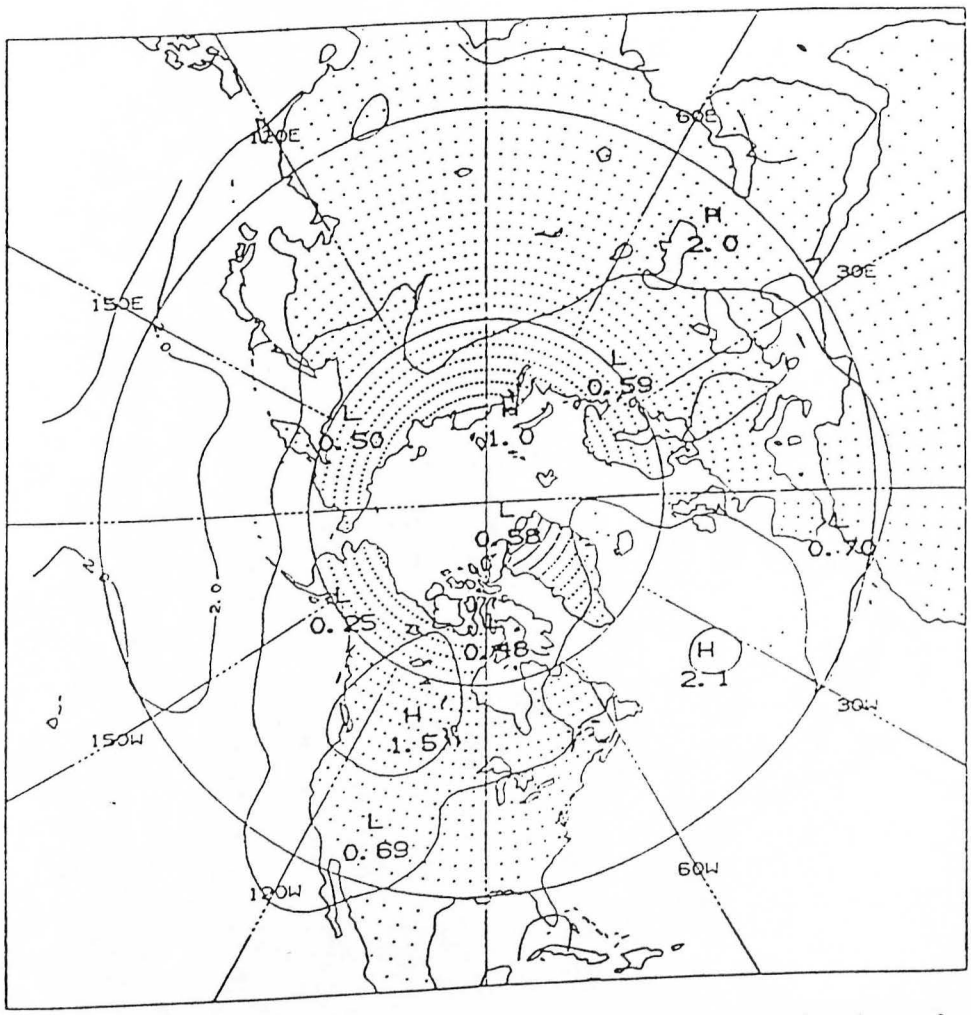

Figure 19: F-statistic values representing the ratio of interannual variance of winter monthly mean to interannual variance due to climatic noise of winter month. Contour interval 1.0.

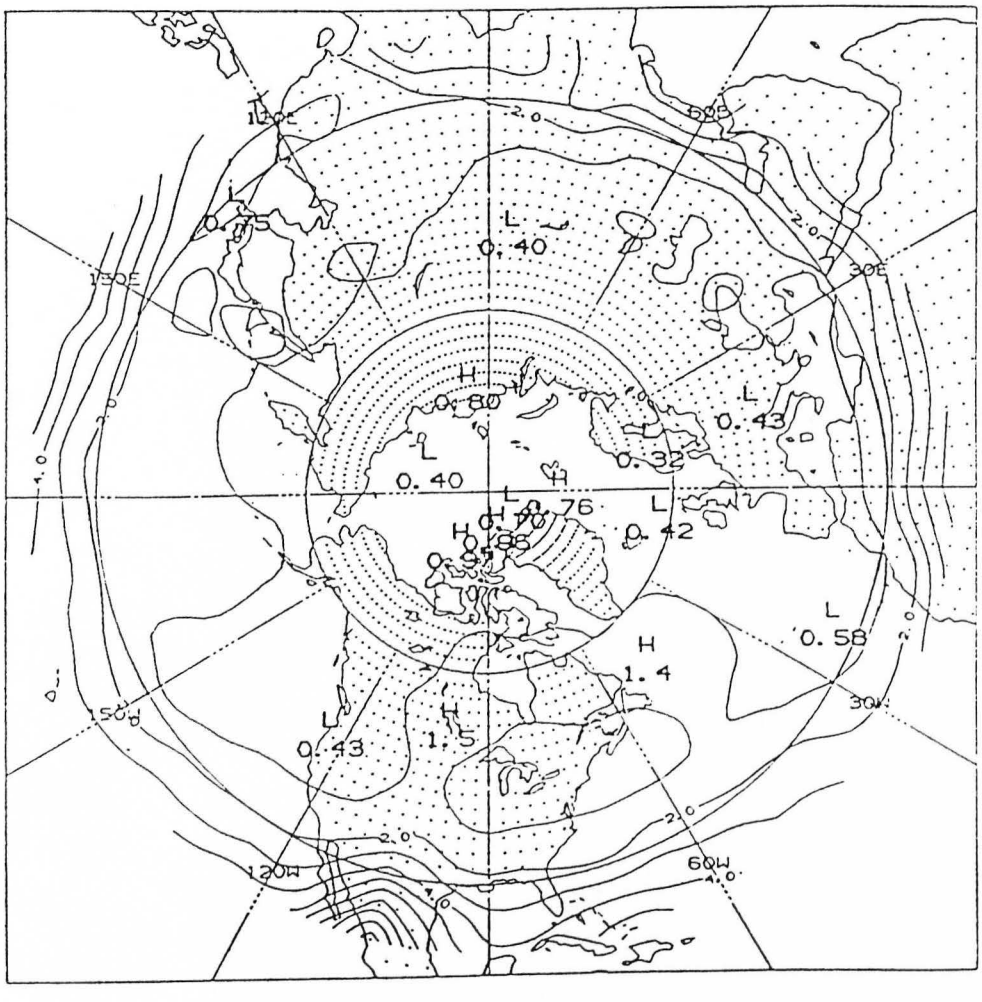

Figure 20: F-statistic values representing the ratio of interannual variance of summer monthly mean to interannual variance due to climatic noise of summer month. Contour interval 1.0.